



Kinetics and mechanisms of congo-red dye removal from aqueous solution using activated *Moringa oleifera* seed coat as adsorbent

Jamiu M. Jabar¹ · Yisau A. Odusote² · Kazeem A. Alabi³ · Ibrahim B. Ahmed¹

Received: 17 June 2019 / Accepted: 30 April 2020 / Published online: 15 May 2020
© The Author(s) 2020

Abstract

Moringa oleifera (MO) seed coat, a postharvest waste of MO seed, was mercerized and used as eco-friendly adsorbent for removal of Congo red (CR) dye from aqueous solution at different time and temperature. Mercerized *M. oleifera* seed coat (MSC) was characterized through scanning electron microscopy (SEM) and Fourier transform infrared spectroscopy (FTIR) before and after adsorption process. Data obtained from effect of contact time on CR dye-uptake were applied on Elovich, pseudo-first- and second-order kinetic models, as well as on intraparticle diffusion and Boyd models. SEM and FTIR showed adsorption of CR dye on MSC through filled holes (SEM), appearance of new and shifting existing of functional groups (FTIR) on the surface of MSC after adsorption process. Adsorption kinetics was seen to be best fitted with pseudo-second-order model with the highest value of correlation coefficient at all temperatures. Film diffusion mechanism controlled the adsorption process, where external mass transfer was higher than internal mass transfer. Adsorption kinetics parameters confirmed removal of CR dye from aqueous solution through chemical and physical adsorption on MSC.

Keywords Adsorption kinetics · Film diffusion · Dye uptake · Model · *Moringa oleifera*

Introduction

Congo red (CR) dye is a disazo synthetic dye, characterized by large molecular structure with two azo group (N=N) that are bond to aromatic rings having linear and planar molecular structure (Dhaif-Allah et al. 2020; Christie 2015; Rong et al. 2015). Presently, synthetic dye covers about 60–70% of total coloring matter used in chemical and allied industries (Cheng et al. 2015). CR dye is used in dye house for coloring textile, pulp/paper, making paint, etc. (due to its intense color, high affinity and fastness properties), (Chen and Zhao 2009) as pH indicator in chemical laboratory and for microbial staining (Chukki et al. 2018). Its effluent from these industries, if not properly treated before being discharged into the water bodies, can cause

severe injury to aquatic habitants and human beings that use water from those receiving water bodies for domestic purpose (Somasekharareddy et al. 2012). The injury to aquatic habitants can be through reduction in phytoplankton photosynthesis and water dissolved oxygen (Fisli et al. 2014). Formation of benzidine by CR dye in receiving water body can cause human cancer of the breast, skin or throat (Chatterjee et al. 2007). Several researchers have tried to remove coloring matter from wastewater by biological (assimilation, enhanced biological dye removal, wastewater stabilization) methods (Aljeboree et al. 2014; Chatterjee and Woo 2010; Hu et al. 2010), photocatalytic degradation (Amaranatha et al. 2015) and chemical (precipitation, coagulation, flocculation, crystallization and ion exchange) methods (Pathania et al. 2017; Babu et al. 2015). Others are physical (microfiltration, reverse osmosis, electrodialysis, magnetic separation and adsorption) methods (Tang et al. 2014). Among all these methods of removal of dye from aqueous solution, adsorption process is seen to be the best method (El Haddad et al. 2013). The frequently used adsorbent in wastewater treatment by adsorption technique is commercial activated carbon (CAC). This was due to its high uptake capacity, high surface area, environment friendly, easy to operate, simple, time saving and non-toxic

✉ Jamiu M. Jabar
jmjabar@futa.edu.ng

¹ Chemistry Department, The Federal University of Technology, P.M.B. 704, Akure, Nigeria

² Physcis Department, The Federal University of Technology, P.M.B. 704, Akure, Nigeria

³ Department of Chemical Sciences, Fountain University, P.M.B 4491, Osogbo, Nigeria

nature (Salleh et al. 2011). Recently, researchers are now finding alternative to the use of CAC in wastewater treatment due to high cost of operation involved (Jabar and Odusote 2020). Some of the synthetic adsorbents tried by some researchers as alternative to CAC are $Zn_{0.3}Fe_{0.45}O_3$ (Jethava and Fegade 2018), modified zeolites (Liu et al. 2014), synthesized MgO (Li 2019) and nano-fiber (Bhau-mik et al. 2013), but high cost, non-biodegradability and regeneration of many of these adsorbents made researchers to be looking into green materials as possible alternative. Plant derived adsorbents seen to be in front line of these alternative to CAC in adsorption technology, probably due to availability at visually no cost and high regeneration ability, besides other desired attributes of CAC (Jabar and Odusote 2020). Some plant materials used as adsorbents for removal of CR dye and other classes of dye from aqueous solution are oil palm empty fruit bunch fiber (Jabar and Odusote 2020), fenugreek seed spent (Dhaif-Allah et al. 2020), groundnut shell (Bayuo et al. 2019), *Moringa oleifera* leaf (Bello et al. 2017), aloe vera leaves wastes (Omidi-Khaniabadi et al. 2016), aloe vera green wastes (Omidi-Khaniabadi et al. 2015), jujuba seeds (Reddy et al. 2012), bagasse (Zhang et al. 2011), rice husk (Han et al. 2008) and *Azadirachta indica* leaf (Bhattacharya and Sharma 2004) to mention just a few. Mercerization of MO seed coat as adsorbent in removal of dye from industrial or simulated effluent has not been reported to the best of our knowledge.

Moringa oleifera (MO) plant is a native of India, presently grown in many parts of the world. In Nigeria, it is grown for food and medicinal purposes (Siddhuraju and Becker 2003). When matured, the plant is 10–13 m in height and 30–35 cm width with brown fruit containing 10–24 seeds. Postharvest of MO seeds generates seed coats as environment waste (Bello et al. 2017). Conversion of this waste to adsorbent for removal of dye from aqueous solution is a good technique for conversion of waste to wealth (Bayuo et al. 2019). The aim of this research is to develop a novel adsorbent from MO seed coat through mercerization process. This adsorbent was used to remove CR dye from aqueous solution, kinetics, and mechanisms of adsorption processes were investigated.

Experimental methods

Materials

MO seed coat was obtained from Itaoniyan road, along old Akure-Ondo road Akure. It was authenticated at Department of Crop, Soil and Pest Management, Federal University of Technology, Akure, Nigeria. CR dye stuff and sodium hydroxide used are Anal reagents obtained from Sigma-Aldrich Chemical, Germany.

Preparation of adsorbent

MO seed coat was washed several times with water to remove adhered impurity, oven-dried at 105 °C to a constant weight and ground with an electrical blender. Purified MO seed coat was chemically activated as described by Ozsin et al. (2019) with slight modification. It was soaked in 5% NaOH solution for 2 h, washed several time with distilled water to neutral pH. Sodium hydroxide-modified MO seed coat was oven-dried at 105 °C to a constant weight to obtain chemically modified *M. oleifera* seed coat (MSC). MSC was then crushed and sieved to particle size between 150–170 µm. This was used for adsorption without any further modification.

Characterization of MSC adsorbent

Scanning electron micrographs (SEM) of the MSC (before and after adsorption process) were taken in an XL 20 Philips SEM. The surface of the fibers was studied with the microscope operated at 10.0 kV. The samples were coated with a 10-nm-thick layer of gold.

Fourier transform infrared spectroscopic (FTIR) method of analysis was used in determination of functional groups in MSC before and after adsorption process. The infrared spectra of the MSC (before and after adsorption process) were obtained by using MSC mixed with potassium bromide at ratio 1:100 in a mortar pestle. The mixture was then taken in a dice of specific dimension to form pellet by pressing with a hand press machine, placed on the sample holder of the IR spectrometer (PerkinElmer) operated at spectral range 4000–500 cm^{-1} .

Other properties of MSC determined are moisture content, ash content, surface area (Sear method) and pH (ASTMD 3838–80).

Preparation and standardization of CR dye liquor

CR dye (10 mg) was accurately weighed into 250 mL conical flask, and distilled water (10 mL) was added to make a paste. The paste was stirred; little more quantity of distilled water was added and stirred for total dissolution of the dye. The dissolved dye solution was transferred into the 1 L standard flask and made up to marked point with distilled water.

The aqueous dye solution was standardized on UV–visible spectrophotometer (Pharmacia LKB Biochrome 4060). Its wavelength at maximum absorption (λ_{max}) was found to be 500 nm, and this was used to measure the absorbance of serially diluted solutions made from stock solution (2, 4,

6, 8, 10 mg/L). Subsequently, absorbance of the dye effluent after each of adsorption processes was measured to provide means of evaluating the percentage dye removed, dye-uptake at particular time and at equilibrium by the adsorbent used.

Impact of contact time on adsorption process

Batch adsorption study was carried out on effect of contact time on dye removal using 20 mL CR dye solution in 100 mL conical flask on water bath shaker at shaking speed of 100 rpm. The adsorption processes were carried between temperature of 301 and 321 K at 10 K interval. Initial dye concentration was 10 mg/L, 0.1 g of adsorbent dosage, and adsorption time was varied from 15–150 min. After each of the adsorption experiments, MSC was separated from dye effluent by centrifugation using centrifuge at room temperature, rotation speed of 5000 rpm for 10 min.

Absorbance of aliquot of dye effluent was read on UV–visible spectrophotometer and concentration interpolated from working graph. The percentage CR dye adsorbed on the surface of MSC was determined by difference of the two concentrations (AlOthman et al. 2013) as shown in Eq. 1.

$$%R = \frac{(C_0 - C_t)}{C_0} \times 100\% \tag{1}$$

The amount of CR adsorbed per unit weight of MSC (dye-uptake (mg/g) at a particular time and at equilibrium (Hameed et al. 2013) was calculated as shown in Eqns. 2 and 3.

$$q_t = \frac{(C_0 - C_t)}{W} \times V \tag{2}$$

$$q_e = \frac{(C_0 - C_e)}{W} \times V \tag{3}$$

where %R is percentage CR dye removed, C_0 is the initial dye concentration (mg/L), C_t and C_e are the concentration of dye effluent after adsorption (mg/L) at particular time and equilibrium, respectively; V is the volume of dye solution (L), W is the weight of adsorbent (g), q_t and q_e are the dye-uptake (mg/g) at a particular time and at equilibrium, respectively.

Adsorption kinetic modeling

A precise design of wastewater treatment plant using adsorption technique requires accurate information on

kinetic rate of removal of pollutants from wastewater. Supplying this information requires treatment of data obtained from effect of contact time on adsorption process. In this work, the data obtained from effect of contact time on quantity of CR dye adsorbed at the surface of MSC were used in Lagergren pseudo-first-order (Eq. 4), pseudo-second-order (Eq. 5) and Elovich kinetic models (Eq. 6) as described by Aljeboree et al. (2014).

$$\log(q_e - q_t) = \log q_e - \left(\frac{k_1}{2.303}\right)t \tag{4}$$

$$\frac{t}{q_t} = \frac{1}{h_2} + \left(\frac{1}{q_e}\right)t \tag{5}$$

where $h_2 = k_2 q_e^2$

$$q_t = \left(\frac{1}{\beta}\right)\ln(\alpha \cdot \beta) + \left(\frac{1}{\beta}\right)\ln(t) \tag{6}$$

where q_e and q_t (mg/g) are dye-uptake at equilibrium and at time t , respectively, k_1 is rate constant of pseudo-first-order adsorption (mg/g min), h_2 is initial adsorption rate (mg/g), k_2 is rate constant of pseudo-second-order adsorption (g/mg), β is extent of surface coverage (min g/mg), α is rate of adsorption (mg/g min) and t is time (min).

Suitability of any of these models to best fit with adsorption process is the closeness of experimented dye-uptake ($q_{e(\text{exp})}$) at equilibrium to calculated dye-uptake ($q_{e(\text{cal})}$) in pseudo-first- and second-order kinetic models. Other factors that determine best suitable kinetic are values of correlation coefficient R^2 and sum of square error SSE (Eq. 7). The higher the value of R^2 and the lower the value of SSE, the more fit the model. N is number of data points (Pura and Atun 2009).

$$SSE = \frac{\sqrt{\sum (q_{e(\text{cal})} - q_{e(\text{exp})})^2}}{N} \tag{7}$$

Arrhenius expression (1889), that linked pseudo-second-order rate constant k_2 to temperature (Eq. 8), can be used to predict type of adsorption process.

$$k_2 = k_0 e^{-E_a/RT} \tag{8}$$

where k_2 is rate constant of pseudo-second-order, k_0 is the frequency factor (gmg⁻¹), R is the gas constant (8.314 J/mol K) and E_a is activation energy for adsorption process (kJ/mol) and T is absolute temperature (K). If the value of $E_a \geq 40$ kJ/mol, the type of adsorption process is chemisorption, but if otherwise it is physisorption (Bannerjee and Chattopadhyaya 2017).

Adsorption mechanism

Mechanism of adsorption process was deduced from intraparticle diffusion (Eq. 9) and Boyd kinetic models (Eqs. 10–13) using data obtained from effect of contact time on adsorption process as described by (Kumar and Kumaran 2005).

$$q_t = k_{id}t^{0.5} + C \quad (9)$$

Intraparticle diffusion was used to determine type of adsorption mechanism in the process. If the graph of q_t Vs $t^{0.5}$ is linear and passes through the origin, it means intraparticle diffusion is rate determining step. If otherwise, it means other mechanism is involved together with intraparticle diffusion (Sartape et al. 2014). Boyd expression in (Eq. 10) generates Eq. 13, which can be used to determine type of mechanism involved (Boyd et al. 1947).

$$F = 1 - \frac{6}{\pi^2} \sum_1^{\infty} \left(\frac{1}{n^2} \right) \exp(-n^2 B_t) \quad (10)$$

$$B_t = -0.499 - \ln(1 - F) \quad (11)$$

$$F = \frac{q_t}{q_e} \quad (12)$$

$$B_t = B(t) + C \quad (13)$$

where q_t and q_e are dye-uptake (mg/g) at time t and equilibrium, respectively, k_{id} is the initial rate of intraparticle diffusion (mg/g min^{1/2}), C is intercept that gives information about thickness of the boundary layer, F is the fraction of dye-uptake and B_t is the mathematical function of F and B is time constant (min⁻¹) gotten from slope of B_t Vs t .

If plot of B_t Vs t is linear and passes through the origin, it indicates that adsorption process is controlled by pore (particle) diffusion mechanism, where internal transport of CR dye is greater than external transport. If it does not pass through the origin, it indicates film diffusion controls adsorption process, where external transport is greater than internal transport (Boyd et al. 1947).

Results and discussion

Characterization of MSC

The SEM image of MSC before adsorption (Fig. 1) shows the presence of holes on its surface. These holes are the available pores at the surface of adsorbent, where CR dye molecules are to be captured from aqueous solution

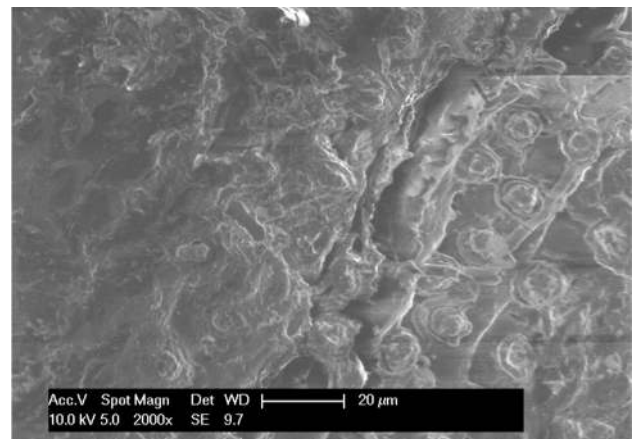


Fig. 1 SEM micrograph of MSC before adsorption of CR dye

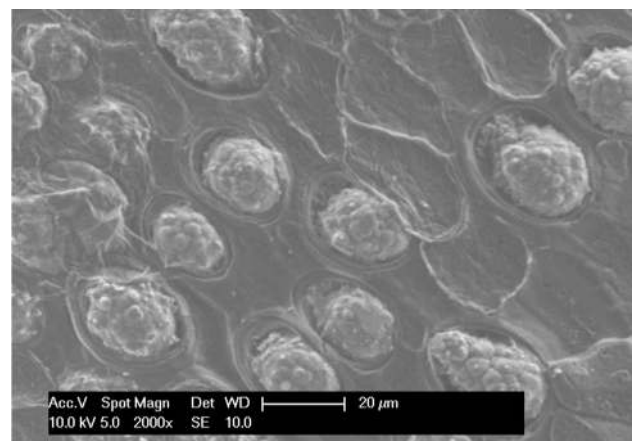


Fig. 2 SEM micrograph of MSC after adsorption of CR dye

(Li 2019). After adsorption process, SEM image of MSC (Fig. 2) displayed the captured dye molecules at the surface of the adsorbent. The captured dye molecules got to fill the available pores in MSC by diffusion of CR dye molecules from aqueous solution to MSC surface through its boundary layer. This was followed by migration of dye molecules from MSC surface to inner pores of the adsorbent and finally adsorbed at the available sites on its surface. The adsorption of CR dye at the surface of MSC might be physical adsorption (physiosorption), through mechanical adhesion of adsorbate on adsorbent. This observation agreed with Boulaiche et al. (2019).

The characteristic functional groups in MSC before and after adsorption of CR from aqueous solution were identified from FTIR spectra in Figs. 3 and 4, respectively. Broad peak at 3271.38 cm⁻¹ indicates the presence of -OH stretching vibration of phenols and alcohols in lignin and cellulose of MSC before adsorption process (Fig. 3). Other peaks in spectrum of MSC before CR dye adsorption are

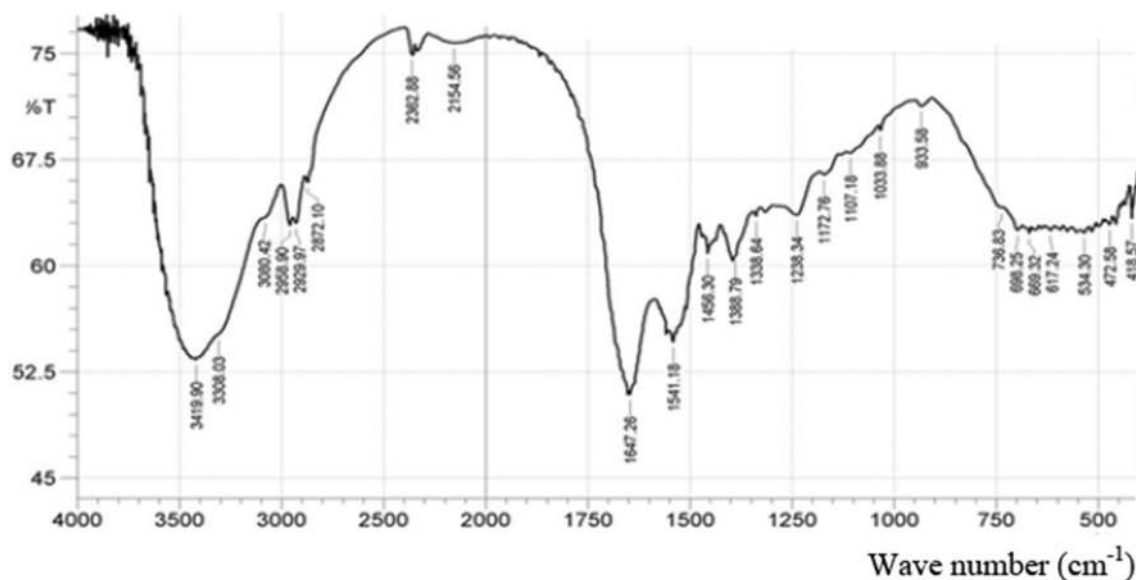


Fig. 3 FTIR spectrum of MSC before adsorption of CR dye

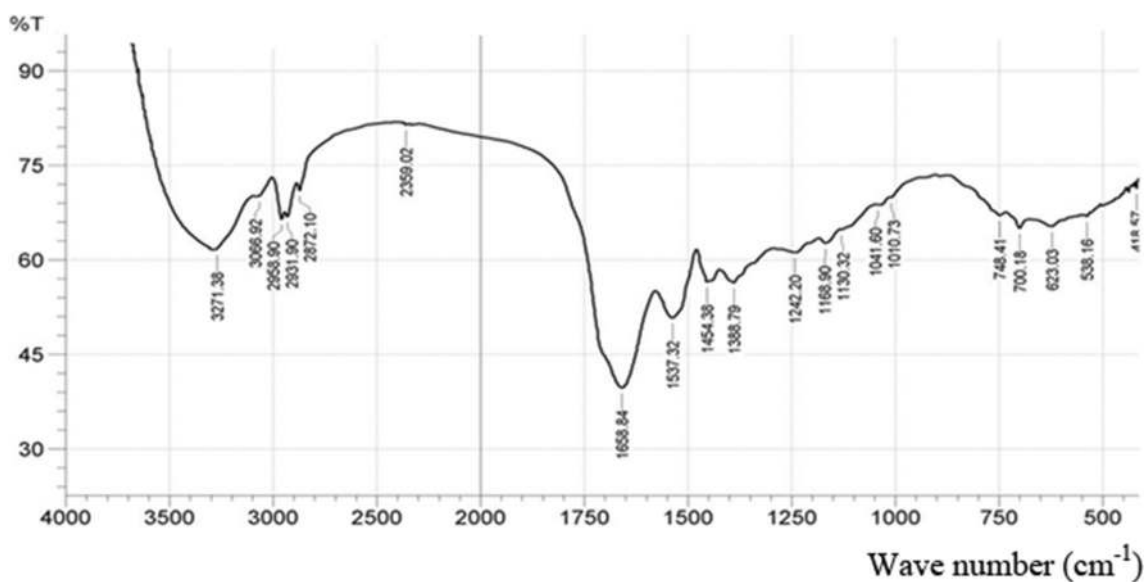


Fig. 4 FTIR spectrum of MSC after adsorption of CR dye

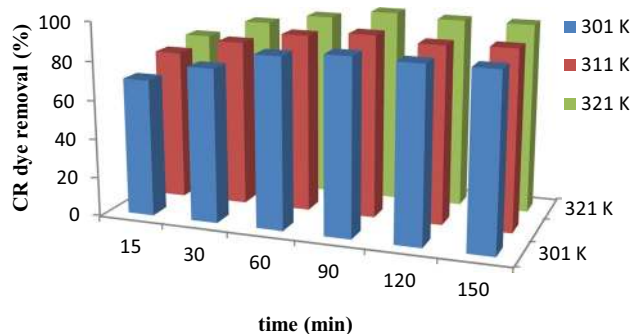
2931.90, 1658.84, 1388.79 and 1041.60 cm^{-1} . These are due to $-\text{CH}_2$, $-\text{C}=\text{C}$, $\text{C}-\text{C}$ and $\text{C}-\text{O}$ stretching, respectively (Bello et al. 2017). MSC spectrum after CR dye adsorption (Fig. 4) has additional peaks at 3419.90, 1172.76 and $698.25\text{--}669.32\text{ cm}^{-1}$. These peaks are due to $-\text{NH}_2$, $\text{C}-\text{N}$ and SO_3^- functional groups in CR dye. These affirmed the removal of CR dye molecules from aqueous solution after adsorption through electrostatic force (chemisorption). The observation is in line with findings made by Li (2019), in combustion synthesis of porous MgO and its adsorption properties. However, the peaks at 3271.38, 2931.90,

1658.84 , 1388.79 and 1041.60 cm^{-1} are shifted to 3308.05, 2958.90, 1647.26, 1388.79 and 1033.88 cm^{-1} , respectively. This shift in absorption bands of MSC after adsorption process suggested the interactions of functional groups in dye molecules with those of MSC adsorbent according to Pathania et al. (2017).

The values of moisture content (MC), ash content (AC), bulk density (BD), surface area (SA) and pH as physico-chemical properties of MSC are shown in Table 1. The literature shows that the acceptable adsorbents for treatment of wastewater have pH value range from 6.0–8.0 (Bello et al.

Table 1 Physicochemical properties of MSC

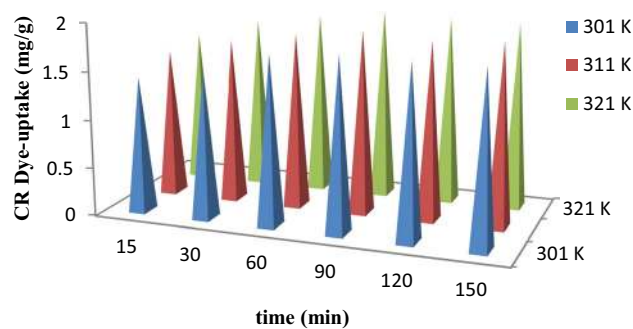
Properties	Results
Moisture content (%)	2.94
Ash content (%)	5.24
Bulk density (gcm^{-3})	0.11 0.11
Surface area (cm^2g)	55.00
pH	7.40

**Fig. 5** Effect of contact time on percentage CR dye removed from aqueous dye solution at different temperatures

2017). The pH value (7.4) of MSC affirmed acceptability of MSC as an alternative adsorbent from biomass for removal of CR dye and related impurities from aqueous solution according Bello et al. (2017). The MC value (low) shows that MSC has a good potential of removing large amount of CR dye from its aqueous solution. Low AC indicated that large amount of volatile matter had been removed during the mercerization process of the adsorbent (Bello and Ahmad 2012). However, the lower the volatile matter, the higher the number of voids/pores in the adsorbent and the higher will be the magnitude of SA (Bello and Semire 2012). The high SA showed that MSC has high potential of dye removal efficiency. The value of BD indicates that large quantity of wastewater that can be treated by the adsorbent, the lower the BD the better the adsorptive potential of the adsorbent (Bello et al. 2011). Hence, low BD value indicated that MSC is a potential adsorbent for removing CR dye from aqueous solution.

Effect of contact time on dye removal and dye-uptake

The quantity of dye removed from aqueous solution by MSC increased as the time of adsorption increases up to 90 min of adsorption process (Fig. 5). After 90 min of adsorption, quantity of CR dye removed declined, this showed that optimum time of adsorption process is 90 min. This observation is in line with Chukki et al. (2018). The rapid increase in

**Fig. 6** Effect of contact time on dye-uptake of CR dye adsorbed from aqueous solution at different temperatures**Table 2** Comparison of optimum contact time of various adsorbents towards CR dye adsorption

Adsorbent	Contact time (min)	References
Zn _{0.3} Fe _{0.45} O ₃ nanoparticle	40	Jethave and Fagade, (2018)
Synthesized MgO	60	Li (2019)
<i>Chrysanthemum indicum</i>	90	Chukki et al. (2018)
Mercerized Moringa seed pod	90	This study

CR dye removal at initial stage up to 90 min might be due to availability of active sites at the surface of MSC. After 90 min of adsorption, vacant active sites got filled up by CR dye molecules; this might cause repulsive force between dye molecule on MSC and those in solution (Etim et al. 2016). The repulsive force might result into reduction in quantity of dye adsorbed after 90 min. This observation is in line with the findings of Deng and Shi (2015) in synthesis and characterization of novel Mg–Al hydrotacite-loaded kaolin clay and its adsorption properties for phosphate in aqueous solution. The same trend of adsorption pattern seen in effect of contact time on dye removal was observed in effect of contact time on dye-uptake (Fig. 6). Optimum contact time for removal of CR dye from aqueous solution using different adsorbent is shown in Table 2. It can be seen from Figs. 5 and 6 that adsorption at 321 K has the highest percentage dye removal/uptake, while that at 301 K has the lowest percentage dye removal/uptake among all the processing temperatures. This might be as a result of increase in kinetic energy of CR dye molecules and efficiency of the adsorbent as temperature increased (Banerjee et al. 2017).

Adsorption kinetic models

Three kinetic models were used to investigate the effect of contact time on CR dye removal from its aqueous solution. These kinetic studies show relationship between the

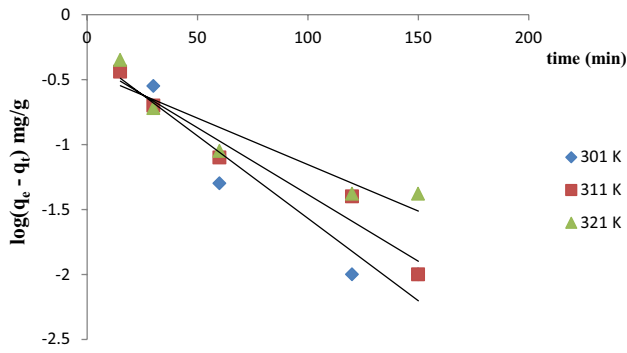


Fig. 7 Pseudo-first-order kinetic plots for adsorption of CR dye on MSC at different temperatures

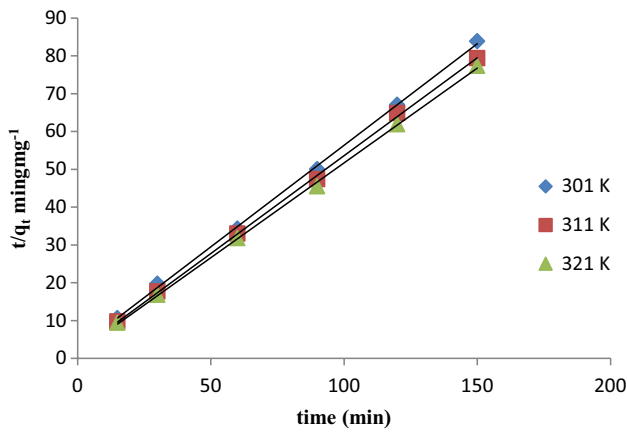


Fig. 8 Pseudo-second-order kinetic plots for adsorption of CR dye on MSC at different temperatures

quantity of adsorbate removed and time of removal from aqueous solution (Yan et al. 2015).

Pseudo-first-order kinetic obeys law of mass action (Hameed et al. 2013), which state that rate of adsorption reaction is proportional to the dye-uptake on the adsorbent from dye solution (Eq. 14).

$$\log \frac{q_t}{d_t} = k_1 (q_e - q_t) \tag{14}$$

where: q_e = Dye-uptake at equilibrium (mg/g), q_t = Dye uptake at a particular time (mg/g), K_1 = pseudo-first-order rate constant ($\text{mgg}^{-1} \text{min}^{-1}$), t = adsorption time (min).

The linearized form of Eq. 14 is shown in Eq. 4. The slope and intercept of graph of $\log(q_e - q_t)Vs t$ (Fig. 7) were used to determine rate constant K_1 and calculated dye-uptake $q_{e,(\text{cal.})}$, respectively.

Pseudo-second-order kinetic shows that the rate of adsorption process is proportional to square of dye-uptake by the adsorbent (Eq. 15) (Chan-Li et al. 2007).

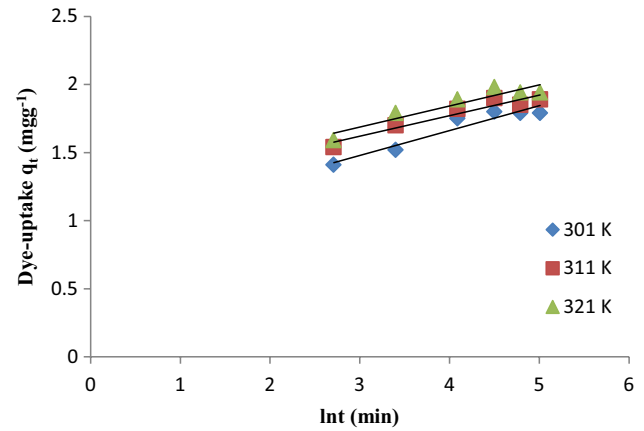


Fig. 9 Elovich kinetic plots for adsorption of CR dye on MSC at different temperatures

Table 3 Kinetic parameters for adsorption of CR dye on MSC at different temperatures

Parameter	Temperature (K)		
	301	311	321
$q_{e(\text{exp.})}$ (mg/g)	1.80	1.90	1.98
Pseudo-first-order kinetic			
$q_{e(\text{cal.})}$ (mg/g)	0.50	0.44	0.32
k_1 ($\text{mgg}^{-1} \text{min}^{-1}$)	2.92×10^{-2}	2.37×10^{-2}	1.62×10^{-2}
R^2	0.9340	0.9539	0.873
SSE (mg/g)	0.22	0.24	0.28
Pseudo-second-order kinetic			
$q_{e(\text{cal.})}$ (mg/g)	1.86	1.93	2.00
k_2 (gmg^{-1})	0.11	0.14	0.16
h_2 (mgg^{-1})	9.18	7.12	6.34
R^2	0.9984	0.9994	0.9994
SSE (mg/g)	0.010	0.005	0.003
Elovich			
B ($\text{mgg}^{-1} \text{min}^{-1}$)	5.47	6.63	6.04
α (min)	30.06	346.52	436.99
R^2	0.9149	0.9117	0.8749
Arrhenius expression			
k_o (gmg^{-1})	2.492.49		
E_a (kJ/mol)	2.01×10^{-3}		
R^2	0.9909		

$$\frac{dq_t}{dt} = k_2 (q_e - q_t)^2 \tag{15}$$

The linearized form of Eq. 15 is shown in Eq. 5. The slope and intercept of graph of $t/q_t Vs t$ (Fig. 8) were used to obtain calculated dye-uptake $q_{e(\text{cal.})}$ and rate constant K_2 , respectively.

The linear form of Elovich equation is shown in Eq. 6. The slope and intercept of the graph of q_t Vs $\ln t$ (Fig. 9) were used to calculate extent of surface coverage β (g/mg) and adsorption rate α (mg/g min). The rate constants, calculated dye-uptake, correlation coefficient and other kinetic constant from the three models studied are presented in Table 3. These calculated kinetic constants indicated pseudo-second-order kinetic with highest correlation coefficient R^2 to fit best. Kinetic does not apply to pseudo-first-order and Elovich model according to Boulaiche et al. (2019). Equally, calculated dye-uptake in pseudo-first-order kinetic is by far less than one obtained from experiment ($q_{e(cal)} \ll q_{e(exp)}$). Whereas, in pseudo-second-order kinetic, the dye-uptake calculated is closer to that obtained from experiment. This further confirms fitness of kinetic studies with pseudo-second-order. This observation agreed with the findings of Hameed et al. (2007) in adsorption of basic dye onto activated carbon prepared from rattan saw dust. The fitness of the models was further tested on values of sum of square error using Eq. 7. It was seen that pseudo-second-order has lower values of SSE (Table 3) indicating kinetic models best fit with pseudo-second-order kinetic and possibility of CR dye adsorption on MSC through chemisorption according to Darwish et al. (2019). Arrhenius expression (Eq. 8) that shows relationship between pseudo-second-order rate constant k_2 and temperature was used to confirm type of adsorption process. The linearized Arrhenius expression (Eq. 16) was used to predict type of adsorption process by plotting $\ln k_2$ Vs T^{-1} (Fig. 10). The slope and intercept of the graph were used to calculate activation energy (E_a) and frequency factor (k_0) of adsorption process, respectively.

$$\ln k_2 = \ln k_0 - \frac{E_a}{R} \left(\frac{1}{T} \right) \tag{16}$$

The activation energy E_a was found to be 2.01 kJ/mol, and frequency factor k_0 was 0.9153. Value of activation energy (E_a) less than 40 kJ/mol shows that adsorption of CR dye

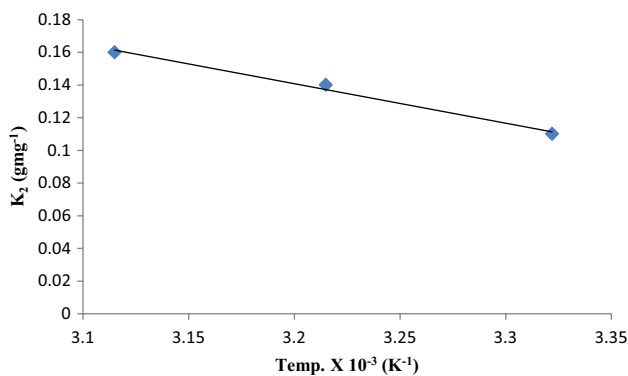


Fig. 10 Arrhenius plot for adsorption of CR dye on MSC

onto MSC might be through physisorption according to Banerjee and Chattopadhyaya (2017). Therefore, one can say that CR dye was removed from aqueous solution using MSC as adsorbent through physiso-chemisorption process.

Mechanism of adsorption kinetic

Two models used to investigate mechanism of adsorption of CR dye removal from its aqueous solution using MSC as adsorbent are intra-particle (Weber–Morris) (Eq. 9) and Boyd diffusion kinetic models (Eqs. 10–13).

Generally, adsorption process is governed by internal or external mass transfer or both (Sartape et al. 2014). Inability of graph of q_t Vs $t^{0.5}$ to pass through the origin (Fig. 11) and value of $C > 0$ (Table 4) indicated that along with intra-particle diffusion other mechanism is involved in adsorption process (Vasanth et al. 2005). Biphasic nature of the graph showed that either film or pore (particle) diffusion is involved in the CR dye adsorption process (Nethaji et al. 2013).

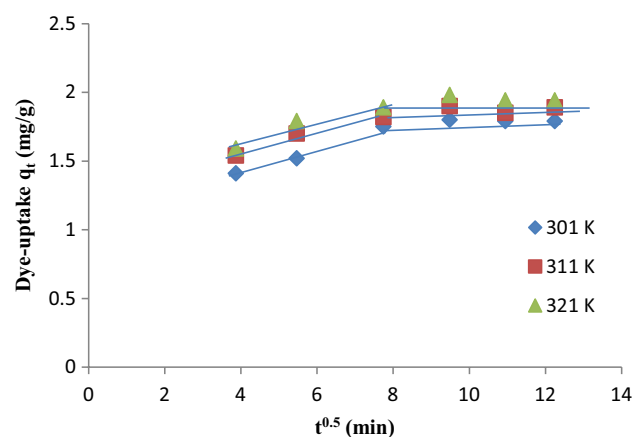


Fig. 11 Intraparticle diffusion plots for adsorption of CR dye on MSC at different temperatures

Table 4 Adsorption mechanism parameters for adsorption of CR dye on MSC at different temperatures

Parameter	Temperature (K)		
	301	311	321
Intraparticle diffusion			
K_{id} (mgg ⁻¹ min ⁻¹)	0.0477	0.0391	0.0394
C (mgg ⁻¹)	1.2809	1.4592	1.5280
R^2	0.8331	0.8183	0.7634
Boyd expression			
B (min ⁻¹)	0.0245	0.0153	0.0166
C	0.8198	1.4533	1.2010
R^2	0.9378	0.8006	0.9154
$D_i \times 10^{-5}$ (cm ² g ⁻¹ min ⁻¹)	0.14	8.85	9.60

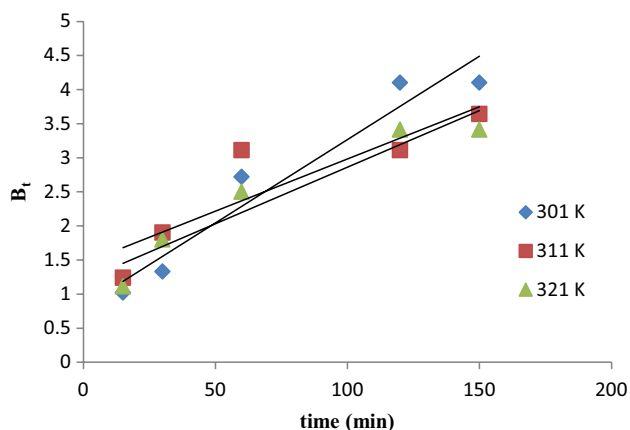


Fig. 12 Boyd kinetic plots for adsorption of CR dye on MSC at different temperatures

Boyd kinetic model was used to confirm either film or pore diffusion was involved in the process. This confirmation was done with the aid of graph of Bt Vs t (Fig. 12). Inability of the linear plot to pass through the origin confirmed the adsorption mechanism is governed by film diffusion mechanism. This indicated that external transport of CR dye is more than internal transport (Sartape et al. 2014).

The slope (B) of B_t Vs t is time constant, which is related to diffusion coefficient D_i in Eqs. 17 and 18 (Kumar et al. 2006).

$$B = \frac{\pi^2}{r^2} D_i \quad (17)$$

$$D_i = \frac{B}{\pi A} \quad (18)$$

The value of B (min^{-1}) was gotten from the slope of B_t Vs t , and surface area A (cm^2/g) was obtained from physicochemical characterization of MSC (Table 1). Values of parameters from adsorption mechanism are presented in Table 4.

The values of effective diffusion coefficient D_i ($\text{cm}^2 \text{g}^{-1} \text{min}^{-1}$) calculated at 301, 311 and 321 K not fallen between 10 and 11 $\text{cm}^2 \text{g}^{-1} \text{min}^{-1}$ are a further confirmation of rate determining step not particle diffusion but film diffusion mechanism (Kumar et al. 2006).

Conclusion

MSC adsorbent was prepared through mercerization of *M. oleifera* seed coat. It was used to investigate removal of CR dye from aqueous solution. SEM characterization indicated surface morphology of MSC to be rough with irregular shape and several pores accounting for physical removal (physisorption) of CR dye from aqueous solution.

FTIR displayed appearance of new peaks at 3419.90, 1172.76 and 698.25–669.32 cm^{-1} on MSC after adsorption process, confirming electrostatic attraction (chemisorption) of CR dye onto MSC through $-\text{NH}_2$, C–N and SO_3^- functional groups, respectively, in CR dye. > 90% of CR dye was removed from aqueous solution at optimum adsorption temperature and contact time 321 K and 90 min, respectively. Adsorption kinetic followed pseudo-second-order model, indicating chemisorption nature of the process and activation energy (E_a) < 40 kJ/mol confirmed inclusion of physisorption in adsorption process. The mechanism of adsorption process showed film diffusion as adsorption rate determining step. Finally, MSC can be considered as an effective alternative adsorbent to CAC for treatment of wastewater polluted by CR dye.

Acknowledgements The authors are highly thankful to the Federal Government of Nigeria for awarding Tertiary Education Trust Fund (2016) grants to Polymer and Textile research group, Department of Chemistry, the Federal University of Technology, Akure (FUTA) where laboratory facilities for the success of this research work were obtained.

Compliance with ethical standards

Conflict of interest The authors hereby declared that we have no competing interest.

Open Access This article is licensed under a Creative Commons Attribution 4.0 International License, which permits use, sharing, adaptation, distribution and reproduction in any medium or format, as long as you give appropriate credit to the original author(s) and the source, provide a link to the Creative Commons licence, and indicate if changes were made. The images or other third party material in this article are included in the article's Creative Commons licence, unless indicated otherwise in a credit line to the material. If material is not included in the article's Creative Commons licence and your intended use is not permitted by statutory regulation or exceeds the permitted use, you will need to obtain permission directly from the copyright holder. To view a copy of this licence, visit <http://creativecommons.org/licenses/by/4.0/>.

References

- Aljeboree AM, Alshirri AN, Alkaim AF (2014) Kinetics and equilibrium study for the adsorption of textile dyes on coconut shell activated carbon. Arab J Chem. <https://doi.org/10.1016/j.arabjc.2014.01.020>
- AlOthman ZA, Habila MA, Ali R, Abdel A, Ghafar MS, Eldin H (2013) Valorization of two waste streams into activated carbon and studying its adsorption kinetics equilibrium isotherms and thermodynamics for methylene blue removal. Arab J Chem 2:2–12. <https://doi.org/10.1016/j.arabjc.2013.05.007>
- Amaranatha RD, Lee S, Choi J, Park S, Ma R, Yang H, Kim TK (2015) Green synthesis of AgI-reduced graphene oxide nanocomposites: toward enhanced visible-light photocatalytic activity for organic dye removal. Appl Surf Sci 341:175–184
- Arrhenius S (1889) Über die reaktionsgeschwindigkeit bei inversion von rohrzucker durch sauren. J Phys Chem 14:226

- Babu SS, Mohandass C, Vijayaraj AS, Dhale AM (2015) detoxification and color removal of congo red by a novel dietzia sp. (dts26)—a microcosm approach. *Ecotoxicol Environ Safety* 114:52–60
- Banerjee S, Chattopahyaya MC (2017) Adsorption characteristics for the removal of a toxic dye, tartrazine from aqueous solutions by low cost agricultural by-product. *Arab J Chem* 10:S1629–S1638. <https://doi.org/10.1016/j.arabjc.2013.06.005>
- Bayuo J, Pelig-Ba KB, Abukari MA (2019) Adsorptive removal of chromium(VI) from aqueous solution unto groundnut shell. *Appl Water Sci* 9:107
- Bello OS, Adegoke KA, Akinyunni OO (2017) Preparation and characterization of a novel adsorbent from *Moringa oleifera* leaf. *Appl Water Sci* 7:1295–1305
- Bello OS, Ahmad MA (2012) Coconut (*Cocos nucifera*) shell based activated carbon for the removal of malachite green dye from aqueous solutions. *Sep Sci Technol* 47:903–912
- Bello OS, Ahmad MA, Siang TT (2011) Utilization of cocoa pod husk for the removal of Remazol Black B reactive dye from aqueous solutions: kinetic, equilibrium and thermodynamic studies. *Trends Appl Sci Res* 6(8):794–812
- Bello OS, Semire B (2012) Equilibrium, kinetic and quantum chemical studies on the adsorption of Congo red using *Imperata cylindrica* leaf powder activated carbon. *Toxicol Environ Chem* 94:1114–1124
- Bhattacharrya K, Sharma A (2004) Azadirachta indica leaf powder as an effective biosorbent for dyes: a case study with aqueous congo red solutions. *J Environ Manag* 71:217–229
- Bhaumik M, McCrindle R, Maity A (2013) Efficient removal of Congo red from aqueous solutions by adsorption onto interconnected polypyrrole-polyaniline nanofibres. *Chem Eng J* 228:506–515
- Boulaiche W, Hamdi B, Trari M (2019) Removal of heavy metals by chitin: equilibrium, kinetic and thermodynamic studies. *Appl Water Sci* 9:39
- Boyd GE, Adamson AW, Myers LS Jr (1947) The exchange adsorption of ions from aqueous solutions by organic zeolites II: kinetics. *J Am Chem Soc* 69:2836
- Chan-Li H, Yu-wen LY, Chil-Chang H, Yao-Hui H, Chunch-Yung C (2007) Adsorption kinetic, thermodynamic and desorption studies of C.I. reactive black 5, on a novel photo assisted fento catalyst. *Dyes Pigm* 75:130–135
- Chatterjee S, Chatterjee S, Chatterjee BP, Guha AK (2007) Adsorptive removal of congo red, a carcinogenic textile dye by chitosan hydrobeads: binding mechanism, equilibrium and kinetics. *Colloids Surf A Physicochem Eng Asp* 299:146–152
- Chatterjee SM, Lee W, Woo SH (2010) Adsorption of congo red by chitosan hydrogel beads impregnated with carbon nanotubes. *Biores Tech* 101:1800–1806
- Chen H, Zhao J (2009) Adsorption study for removal of congo red anionic dye using organo-attapulgite. *Adsorption* 15:381–389
- Cheng Z, Zhang L, Guo X, Jiang X, Li T (2015) Adsorption behavior of direct red 80 and congo red onto activated carbon/ surfactant: process optimization, kinetics and equilibrium. *Spectrochim Acta Part A Mol Biomol Spectrosc* 137:1126–1143
- Christie RM (2015) Colour chemistry, 2nd edn. The Royal Society of Chemistry, Cambridge
- Chukki J, Abinandan S, Shanthakumar S (2018) Chrysanthemum indicum microparticles on removal of hazardous congo red using response surface methodology. *Int J Ind Chem* 9:305–316
- Darwish AAA, Rashad M, Al-Aoh HA (2019) Methyl orange adsorption comparison on nanoparticles: Isotherm, kinetics and thermodynamic studies. *Dyes Pigm* 160:563–571
- Deng L, Shi Z (2015) Synthesis and characterization of a novel Mg-Al hydrotalcite-loaded kaolin clay and its adsorption properties for phosphate in aqueous solution. *J Alloys Comp* 637:188–196
- Dhaif-Allah MAH, Taqui SN, Syed UT, Syed AA (2020) Kinetic and isotherm modeling for acid blue adsorption onto low-cost nutritional industrial fenugreek seed spent. *Appl Water Sci* 10:58. <https://doi.org/10.1007/s13201-20-1141-3>
- Etim UJ, Umoren SA, Eduok UM (2016) Coconut coir dust as low cost adsorbent for the removal of cationic dye from aqueous solution. *J Saudi Chem Soc* 20:S67–S76
- El Haddad M, Slimani R, Mamouni R, ElAntri S, Lazar S (2013) Removal of two textile dyes from aqueous solutions onto calcined bones. *J Assoc Arab Uni Basic Appl Sci* 14:51–59. <https://doi.org/10.1016/j.jaubas.2013.03.002>
- Fisli A, Yusuf S, Ridwan YK, Krisnandi JG (2014) Preparation and characterization of magnetite-silica nano-composite as adsorbents for removal of methylene blue dyes from environmental water samples. *Adv Mater Res* 896:525–531
- Hameed BH, Almad AL, Latiff KNA (2007) Adsorption of basic dye (methylene blue) onto activated carbon prepared from rattan sawdust. *Dyes Pigm* 75:143–149
- Hameed KS, Muthirulan P, Meenakshi SM (2013) Adsorption of chromotrope dye onto activated carbons obtained from the seeds of various plants: equilibrium and kinetics studies. *Arab J Chem*. <https://doi.org/10.1016/j.arabjc.2013.07.058>
- Han R, Ding D, Xu Y, Zou W, Wang Y, Li Y, Zou L (2008) Use of rice husk for the adsorption of congo red from aqueous solution in column mode. *Biores Tech* 99:2938–2946
- Hu Z, Chen H, Ji F, Yuan S (2010) Removal of congo red from aqueous solution by cattail root. *J Hazard Mater* 173:292–297
- Jabar JM, Odusote YA (2020) Removal of cibacron blue 3G-A (CB) dye from aqueous solution using chemo-physically activated biochar from oil palm empty fruit bunch fiber. *Arab J Chem*. <https://doi.org/10.1016/j.arabjc.2020.03.020>
- Jethava G, Fegade U (2018) Design and synthesis of Zn_{0.3}Fe_{0.45}O₃ nanoparticle for efficient removal of congo red dye and its kinetic and isotherm investigation. *Int J Ind Chem* 9:85–97
- Kumar KV, Kumaran A (2005) Removal of Methylene blue by mango seed kernel powder. *Biochem Eng J* 27:83–93
- Kumar KV, Ramamurthi V, Sivanesan S (2006) Biosorption of malachite green, a cationic dye onto *Pithophora* sp., a fresh water algae. *Dyes Pigm* 69:102
- Li S (2019) Combustion synthesis of porous MgO and its adsorption properties. *Int J Ind Chem* 10:89–96. <https://doi.org/10.1007/s40090-019-0174-7>
- Liu S, Ding Y, Li P, Diao K, Tan X, Lei F, Zhan Y, Li Q, Huang B, Huang Z (2014) Adsorption of the anionic dye Congo red from aqueous solution onto natural zeolites modified with *N,N*-dimethyl dehydroabietylamine oxide. *Chem Eng J* 248:135–144
- Nethaji S, Sivasamy A, Mandal AB (2013) Adsorption isotherms, kinetics and mechanism for the adsorption of cationic and anionic dyes onto carbonaceous particles prepared from *Juglans regia* shell biomass. *Int J Environ Sci Technol* 10:231–242
- Omidi-Khaniabadi Y, Heydari R, Nourmoradi H, Basiri H, Basiri H (2016) Low-cost sorbent for the removal of aniline and methyl orange from liquid-phase: aloe vera leaves wastes. *J Taiwan Inst Chem Engr* 68:90–98
- Omidi-Khaniabadi Y, Jafari A, Nourmoradi H, Taheri F, Saeedi S (2015) Adsorption of 4-chlorophenol from aqueous solution using activated carbon synthesized from aloe vera green wastes. *J Adv Environ Health Res* 3:120–129
- Ozsin G, Kilic M, Apaydin-Varol E, Putun AE (2019) Chemically activated carbon production from agricultural waste of chickpea and its application for heavy metal adsorption: equilibrium, kinetic, and thermodynamic studies. *Appl Water Sci* 9:56
- Pathania D, Sharma S, Singh P (2017) Removal of methylene blue by adsorption onto activated carbon developed from *Ficus carica* Bast. *Arab J Chem* 10:S1445–S1451

- Pura S, Atun G (2009) Adsorptive removal of acid Blue 113 and tartrazine by fly ash from single and binary dye solutions. *J Sep Sci Technol* 44:75
- Reddy M, Sivaramakrishna L, Reddy A (2012) The use of an agricultural waste material, jujuba seeds for the removal of anionic dye (congo red) from aqueous medium. *J Hazard Mater* 203–204:118–127
- Rong X, Qiu F, Qin J, Zhao H, Yan J, Yang D (2015) A facile hydrothermal synthesis, adsorption kinetics and isotherms to Congo Red azo-dye from aqueous solution of NiO/grapheme nanosheets adsorbent. *J Ind Eng Chem* 26:354–363
- Salleh MAM, Mahmoud DK, Karim WA, Idris A (2011) Cationic and anionic dye adsorption by agricultural solid wastes: a comprehensive review. *Desalination* 280:1–13
- Sartape AS, Mandhare AM, Jadhav VV, Raut PD, Anuse MA, Kolekar SS (2014) Removal of malachite green dye from aqueous solution with adsorption technique using *Limonia acidissima* (wood apple) shell as low cost adsorbent. *Arab J Chem*. <https://doi.org/10.1016/j.arabjc.2013.12.019>
- Siddhuraju P, Becker K (2003) Antioxidant properties of various solvent extract of total phenolic constituents from different agroclimatic origins of drumstick tree (*Moringa oleifera Lam*) leaves. *J Agric Food Chem* 51(8):2144–2155
- Somasekharareddy MC, Sivaramakrishna L, Varadareddy A (2012) The use of an agricultural waste material, Jujuba seeds for the removal of anionic dye (Congo red) from aqueous medium. *J Hazard Mater* 203–204:118–127
- Tang L, Cai Y, Yang G, Liu Y, Zeng G, Zhou Y, Li S, Wang J, Zhang S, Fang Y, He Y (2014) Cobalt nanoparticles-embedded magnetic ordered mesoporous carbon for highly effective adsorption of rhodamine B. *Appl Surf Sci* 314:746–753
- Vasanth KK, Ramamurthi V, Sivanesan S (2005) Modeling the mechanism involved during the sorption of methylene blue onto fly ash. *J Colloid Interface Sci* 284:14–21
- Yan L, Shan R, Yan T, Wei J, Yu S, Yu H, Du B (2015) Kinetic, isotherm and thermodynamic investigations of phosphate adsorption onto core-shell Fe_3O_4 @LDHs composites with easy magnetic separation assistance. *J Colloid Interface Sci* 448:508–516
- Zhang Z, Moghaddam L, O'Hara IM, Doherty WOS (2011) Congo red adsorption by ball-milled sugarcane bagasse. *Chem Eng J* 178:122–128

Publisher's Note Springer Nature remains neutral with regard to jurisdictional claims in published maps and institutional affiliations.